P3.7 ASSESSMENT OF RADIATION OPTIONS IN THE ADVANCED RESEARCH WRF WEATHER FORECAST MODEL

Michael J. Iacono * and Thomas R. Nehrkorn
Atmospheric and Environmental Research, Inc., Lexington, Massachusetts

1. INTRODUCTION

The Advanced Research Weather Research and Forecasting (WRF) model is a widely used meso-scale dynamical model used for weather forecasting and atmospheric research. It incorporates numerous options for physical parameterizations of convection, radiation, cloud microphysics and other processes, which can be selected by the user for particular applications. This work compares the various options for longwave and shortwave radiative transfer available in WRF version 3.1.1 and evaluates their impact on surface downward radiative fluxes and cloud fractions relative to observations for several multi-day forecasts.

2. MODELS AND SIMULATIONS

The RRTMG longwave and shortwave broadband, correlated k-distribution radiation models (Iacono et al., 2008) developed at AER, Inc. were initially implemented as WRF radiation options in 2009. The improved accuracy of these models, which were developed for application to general circulation models (GCMs) for the Department of Energy (DOE) Atmospheric System Research program, is traceable to measurements through their comparison to higher resolution, data-validated line-by-line models (Clough et al., 2005) RRTMG also utilizes the Monte-Carlo Independent Column Approximation, McICA (Barker et al., 2002; Pincus et al., 2003), which is an efficient, statistical method for representing sub-grid scale cloud variability including cloud overlap. RRTMG/McICA was utilized in WRF for this project, though McICA has no effect in situations where only binary clouds (either clear sky or overcast) are present. The relatively fine horizontal grid spacing (of order 10 km) typically used in WRF simulations makes it more likely that a diagnosed cloud will completely fill a grid-box, though fractional cloudiness is generally not prohibited. Since the treatment of cloud overlap is trivial in fully overcast clouds, the McICA approach is only active within RRTMG in the presence of fractional cloud cover. More information about the AER models is available at the AER radiative transfer web site (rtweb.aer.com).

WRF simulations were performed using the WRF-ESG script system developed at AER, which automates the necessary pre-processing and runs WRF in hindcast mode using historical reanalysis data as input to the model. The ESG system automatically downloads input data for a requested time period and prepares it for assimilation into WRF. Input datasets currently supported by the system include the NCEP/NCAR Reanalysis (NNRP; Kalnay et al., 1996) and the North American Regional Reanalysis (NARR; Mesinger et al., 2006). NARR reanalysis data were utilized in this work both to initialize simulations and to provide input for continual data assimilation during each forecast. Simulations with WRF (using various radiative transfer options) were performed for two ten-day periods: 1-10 January 2004 and 1-10 July 2004 for a 40-km grid over North America centered over the United States. Forecasts were performed as a 10-day sequence of 30-hour forecasts starting at the beginning of each calendar day (00 UTC) in the forecast. The grid was selected to include a grid box over northern Oklahoma that overlapped close to the location of the DOE Atmospheric Radiation Measurement (ARM) Southern Great Plains (SGP) facility, which provided the surface measurements used to evaluate the model forecasts.

3. SURFACE MEASUREMENTS

WRF simulations of surface longwave and shortwave fluxes, surface temperature and cloud fraction are compared to observations from the ARM Climate Modeling Best Estimate (CMBE; Xie et al., 2010) data product for the SGP site. The CMBE dataset, which was assembled from multiple ARM measurement sources, provides a time-series of measurement products related to clouds and radiation for SGP, the Tropical Western Pacific (TWP) and North Slope of Alaska (NSA) locations. CMBE cloud-radiation (CLDRAD) products include profiles of cloud fraction, cloud

* *Corresponding author address*: Michael J. Iacono, Atmospheric and Environmental Research, Inc., 131 Hartwell Avenue, Lexington, MA 02421-3105; E-mail: miacono@aer.com.

liquid water path and precipitable water as well as surface and top of the atmosphere radiative fluxes. Additional CMBE atmospheric profile (ATM) products, which are presently only available for SGP, include profiles and surface values for temperature, humidity and winds as well as surface sensible and latent heat and precipitation.

4. WRF RADIATION ASSESSMENT

An assessment of radiative fluxes from the various radiation options in WRF shows that surface flux differences among the options can be significant. In clear sky conditions, this can result from algorithmic differences in the treatment of gaseous absorption and emission in the longwave or extinction (absorption plus scattering) in the shortwave. Discrepancies among the radiation options in the defined concentrations of some trace gases, carbon dioxide in particular, are also present that will impact the resulting fluxes. Finally, substantial flux differences in total sky conditions result from significantly deficient cloud fraction amounts relative to measurements and possible from differences in the parameterizations of cloud fraction. The radiation codes are assessed as they are implemented in WRF without further modification to remove such discrepancies, since the objective is to evaluate the codes they way they are most likely to be used in WRF simulations, that is, without modification.

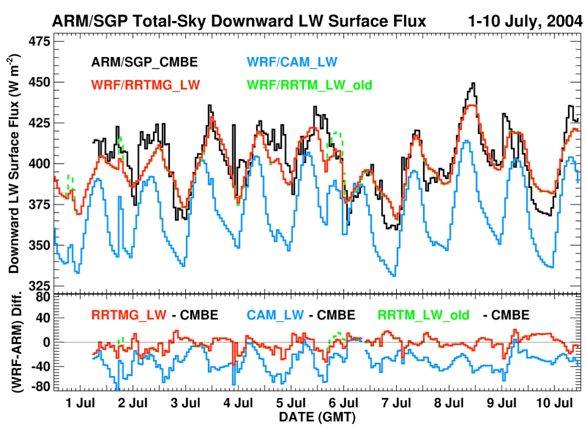

Figure 1. Hourly total-sky downward longwave surface flux at the ARM SGP site for 1-10 July 2004 simulated by WRF using three different longwave radiation models (top) with the ARM CMBE measurement (in black). Model to measurement differences are shown in the bottom panel. Dates are marked at 1200 GMT (12Z UTC) on each day.

The WRF radiation options assessed here include the recently implemented RRTMG longwave and shortwave models, an earlier version of the AER longwave model (RRTM_LW), the NCAR CAM longwave and shortwave models, the NASA Goddard shortwave model, and the Dudhia shortwave model. RRTMG uses the same cloud fraction parameterization based on the relative humidity that provides cloud fraction for the CAM radiation option. Clouds are input to the older RRTM_LW code in binary form, i.e. the grid box is either clear or overcast, with the latter condition occurring when the cloud water path exceeds a threshold value. All experiments used the Purdue Lin microphysics scheme in WRF.

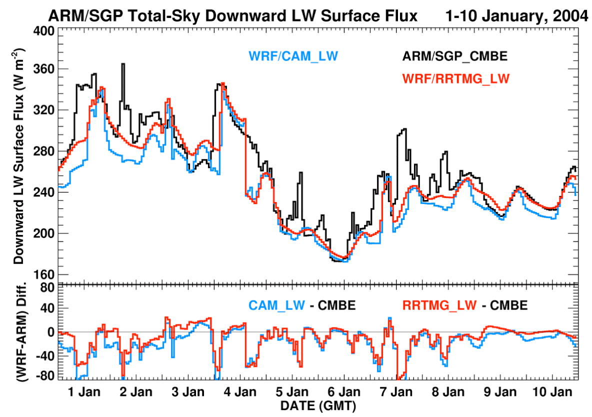

Figure 2. Hourly total-sky downward longwave surface flux at the ARM SGP site for 1-10 January 2004 simulated by WRF using two different longwave radiation models (top) with the ARM CMBE measurement (in black). Model to measurement differences are shown in the bottom panel.

A comparison of hourly, total sky, downward longwave surface flux for 1-10 July 2004 from ten-day WRF forecasts using three different longwave radiation options is shown in the top panel of Figure 1 for a grid box nearest the ARM SGP site. Each simulation used the RRTMG shortwave model. The ARM CMBE hourly measurement of downward longwave surface flux is shown in black in Figure 1. Flux differences between RRTMG_LW (red) and RRTM_LW_old (green) in several time periods are due to the differing cloud specifications, with each producing a substantially different result from the CAM_LW model over this time. Model to measurement differences are shown in the bottom panel of Figure 1. A similar comparison for the same location for the 10-day period from 1-10 January 2004 is shown in Figure 2. Results for the LW models indicated are more similar to each other than during the July period. Although each model is close to the observation in some time periods, significant departures from the measurement are apparent at other times that are primarily related to the specification of clouds.

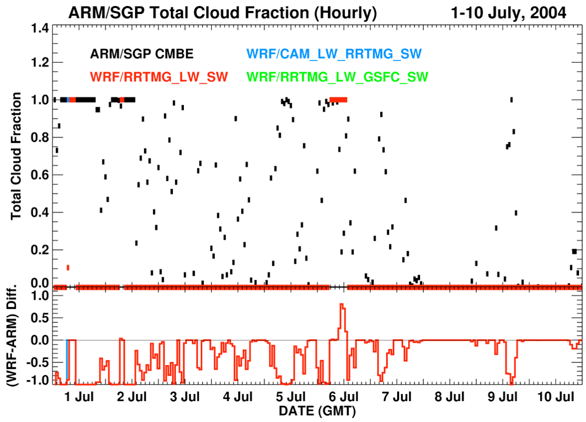

Figure 3. Hourly cloud fraction at the ARM SGP site for 1-10 July 2004 simulated by WRF using three combinations of LW and SW models (top) with the ARM CMBE measurement (in black). Model to measurement differences are shown in the bottom panel.

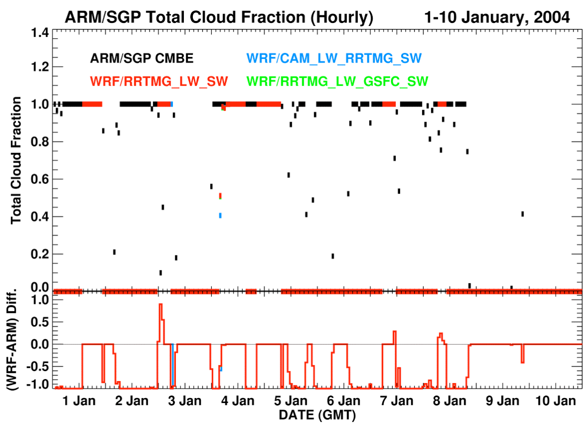

Figure 4. Hourly cloud fraction at the ARM SGP site for 1-10 January 2004 simulated by WRF using three combinations of LW and SW models (top) with the ARM CMBE measurement (in black). Model to measurement differences are shown in the bottom panel.

Cloud fractions simulated by WRF were significantly lower than the measured clouds for the location and time periods shown in Figures 1 and 2, and this greatly affects the simulation of downward longwave surface flux. Figure 3 shows the hourly cloud fraction simulated by WRF using three combinations of LW and SW radiation options (RRTMG_LW and SW in red, CAM_LW and RRTMG_SW in blue, and RRTMG_LW and Goddard SW in green) along with the ARM CMBE measurement (in black) for the 1-10 July 2004 period. The modeled results overlap each other nearly completely, and each model combination produces very little cloud cover during this with time except for a few hours of overcast cloud. The observation, by contrast, has substantially more frequent periods of fractional cloudiness during this time. Model to measured cloud fraction differences are shown in the bottom panel of Figure 3. Simulated and observed hourly cloud fractions for 1-10 January 2004 are shown in Figure 4. Correlations are apparent between periods with longwave downward surface flux errors and large deficiencies in cloud cover (e.g. the period from 04 UTC to 12 UTC on 5 Jul 2004; see Figures 1 and 3). During times with little observed or simulated cloud the simulated longwave downward surface fluxes are in better agreement with observation (e.g. 9-10 January 2004; see Figures 2 and 4). Additional research will be required to establish the cause and extent of the deficient WRF-simulated cloud fractions seen in these experiments.

The cloud amount discrepancies have similar consequences for shortwave fluxes. Hourly, total sky downward shortwave surface fluxes simulated by WRF with three shortwave models (RRTMG_SW in red, Goddard SW in green, and Dudhia SW in orange) are shown in Figure 5 for 1-10 July 2004. At the peak of each diurnal cycle, the Goddard SW model produces downward shortwave surface fluxes that are about 30 Wm^{-2} higher than RRTMG_SW, while the Dudhia SW flux as about 5 Wm^{-2} higher than RRTMG_SW. Model to measurement differences can be substantial for each model, depending on the presence or absence of modeled cloud fraction. The clearest interval near the peak of a diurnal cycle in this period occurs close to and a few hours following 16 UTC on 8 Jul 2004, when each model produces downward shortwave surface fluxes that are relatively close to measurement.

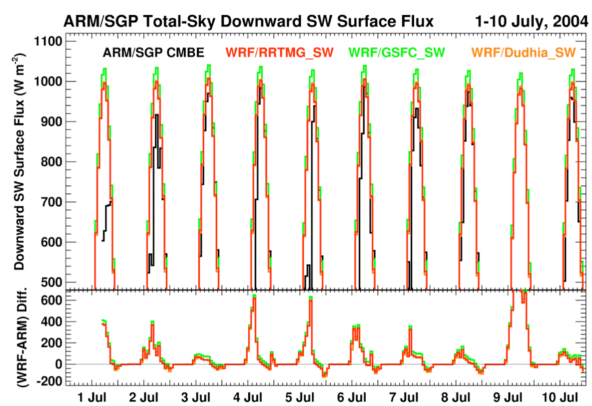

Figure 5. Hourly total-sky downward shortwave surface flux at the ARM SGP site for 1-10 July 2004 simulated by WRF using three different shortwave radiation models (top) with the ARM CMBE measurement (in black). Model to measurement differences are shown in the bottom panel.

5. IMPACT OF RADIATION FREQUENCY

The computational expense of the radiative transfer is among the highest of any components in a dynamical model, and this consideration can be as important as the accuracy of the radiation. WRF permits the user to vary the frequency of the radiation calculation, with potentially large consequences for the overall computational expense of the simulation, though the impact of this change on accuracy may not be widely known. Results in Figures 1-5 are for a radiation frequency of 30 minutes for all models. Figure 6 illustrates the effect on downward longwave surface flux at the ARM SGP site for 1-10 July 2004 in a WRF simulation using RRTMG at five different radiation frequencies: 10, 20, 30, 60 and 120 minutes. There is little effect on this parameter for radiation frequency of 30 minutes or less, while longer frequencies produce increasingly larger differences of up to 7 Wm^{-2} for 60 minutes and up to 15 Wm^{-2} for 120 minutes.

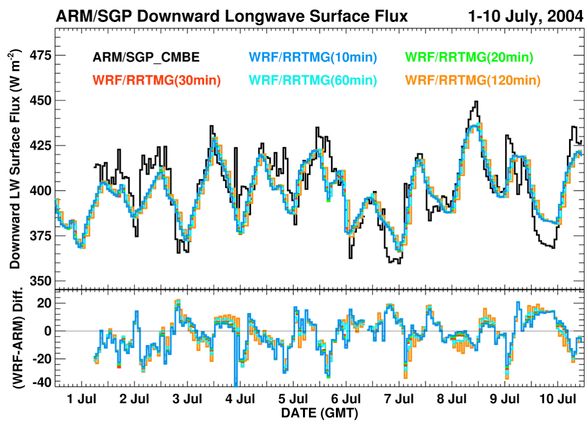

Figure 6. Hourly total-sky downward longwave surface flux at the ARM SGP site for 1-10 July 2004 simulated by WRF using RRTMG longwave and shortwave at five different radiation frequency intervals from 10 minutes to 2 hours (top) with the ARM CMBE measurement (in black). Model to measurement differences are shown in the bottom panel.

6. CONCLUSIONS

Ten-day WRF simulations were performed to examine the impact of the various radiation options relative to ARM Climate Model Best Estimate measurements at the SGP site. Significant differences in hourly surface fluxes relative to observations are present that may be due either to differences in the algorithmic accuracy of each radiation code, or to differences in the treatment or concentration of trace gases, which vary among the radiation options. The largest flux errors occur due to large discrepancies in the modeled cloud fraction in the simulations compared to cloud measurements. Hourly longwave surface flux differences of up to 50 Wm^{-2} occur depending on the radiation option and the modeled cloud fraction. Much larger shortwave surface flux discrepancies occur if clouds are deficient during the diurnal peak in solar heating. It has been shown that the frequency of the radiation calculation has a modest impact of a few Wm-2 on surface fluxes for intervals of 30 minutes or less and up to 5-15 Wm^{-2} for intervals of 1 to 2 hours. However, the accuracy of the radiative transfer is also sensitive to the accuracy of the atmospheric state input to the radiation calculation and to the specification of cloud properties and cloud amount in particular, which requires further evaluation in the WRF model.

7. ACKNOWLEDGMENTS

This work was supported by the Department of Energy Atmospheric System Research program under grant DE-FG02-92ER61549.

8. REFERENCES

Barker, H. W., R. Pincus, and J.-J Morcrette, 2002: The Monte Carlo Independent Column Approximation: Application within Large-Scale Models. In Proceedings of the *GCSS-ARM Workshop on the Representation of Cloud Systems in Large-Scale Models*, May 2002, Kananaskis, AB, Canada.

Clough, S.A., M.W. Shephard, E.J. Mlawer, J.S. Delamere, M.J. Iacono, K. Cady-Pereira, S. Boukabara, P.D. Brown, 2005: Atmospheric radiative transfer modeling: a summary of the AER codes, *J. Quant. Spectrosc. Radiat. Transfer*, **91**, 233-244.

Iacono, M.J., J.S. Delamere, E.J. Mlawer, M.W. Shephard, S.A. Clough, and W.D. Collins, 2008: Radiative forcing by long-lived greenhouse gases: calculations with the AER radiative transfer models, *J. Geophys. Res.*, **113**, D13103, doi:10.1029/2008 JD009944.

Kalnay et al., 1996: The NCEP/NCAR 40-year reanalysis project, *Bull. Amer. Meteor. Soc.*, **77**, 437-470.

Mesinger, F., and co-authors, 2006: North American Regional Reanalysis, *Bull. Amer. Meteor. Soc.*, **87**, 343-360.

Pincus, R., H. W. Barker, J.-J. Morcrette, 2003: A fast, flexible, approximate technique for computing radiative transfer in inhomogeneous cloud fields, *J. Geophys. Res.*, **108**, D13.

Xie, S., and coauthors, 2010: ARM Climate Modeling Best Estimate Data, A new data product for climate studies, *Bull. Amer. Meteor. Soc.*, **91**, 13-20.